Simulation-based occupancy estimation in office buildings using CO_2 sensors

Filip Jorissen[1,3], Wim Boydens[2,4], Lieve Helsen[1,3]
[1]KU Leuven, Leuven, Belgium
[2]UGent, Ghent, Belgium
[3]EnergyVille, Genk, Belgium
[4]Boydens engineering, Groot-Bijgaarden, Belgium

Abstract

Occupancy profiles are required to estimate internal gains in buildings for a model predictive controller. Literature discusses many approaches but the practical usability of these approaches is unclear. A simple dynamic model using only existing sensors from a real office building with 23 zones was tested. A validated Modelica air flow model that computes the mass flow rates required for the occupancy estimation algorithm is also demonstrated. The variable air volume model is published open-source. Limitations of automatic baseline calibration were identified and an alternative CO_2 sensor calibration approach is presented. The occupancy estimation algorithm is validated using measurement data.

Introduction

Pérez-Lombard et al. (2008) estimated that HVAC represents 20% of the total energy use in the USA. Demand controlled ventilation and more advanced control strategies like Model Predictive Control (MPC) allow reducing the energy use of ventilation systems and other HVAC systems. To assess the impact of these control strategies by simulations, building occupancy profiles need to be known approximately, especially when whole-building model validation is required. A non-intrusive, simple and low-cost occupancy estimation technique is desirable in these cases.

Building occupants exhale CO_2, which locally increases the CO_2 concentration. Building Management Systems (BMS) often measure this CO_2 concentration to serve as an input for their control strategies. Since this measurement data is available, it may be used to determine the building occupancy profiles.

Literature describes a *dynamic detection algorithm* (Wang et al., 1999) that estimates occupancy using CO_2 measurements. The algorithm is dynamic since the dynamics of the CO_2 mass balance are taken into account. These dynamics are described by

$$\frac{\mathrm{d}\,c}{\mathrm{d}\,t} = \frac{(c_{ext} - c) \cdot \frac{\dot{m}}{\rho_{air}} + \dot{V}_c \cdot 10^6}{V} \tag{1}$$

where c [ppm] is the indoor CO_2 concentration, c_{ext} [ppm] is the CO_2 concentration of the exterior air, V [m^3] is the zone air volume, $\dot{V}$ [m^3/s] is the volumetric flow rate of the air entering and leaving the zone, ρ_{air} [kg/m^3] is the zone air density and $\dot{V}_c = nG$ [m^3/s] is the total CO_2 generation by n occupants where G is the CO_2 generation rate.

The time derivative of this Ordinary Differential Equation (ODE) is often discretised and then solved for n to find the occupancy of the zone. This approach was used by (Wang et al., 1999; Calì et al., 2015; Ebadat et al., 2015; Mumma, 2004).

Wang et al. (1999) used CO_2 measurements to determine the occupancy by inverting Equation (1). They needed to apply additional filtering to avoid large occupancy swings due to measurement errors. Mumma (2004) performed similar work. Calì et al. (2015) computed the presence of no, one, two or more occupants for several relatively small zones using a model that was calibrated using measured occupancy data. Ansanay-Alex (2013) derived the presence of zero or many occupants based on the slope of the CO_2 measurement, but did not compute how many occupants are present. Ebadat et al. (2015) proposed an occupancy estimation algorithm for a multi-zone building. The approach requires training data for one zone, uses this to fit three model parameters and then rescales these parameters to other zones. Han et al. (2012) combined a distributed sensor network with a statistical estimation method to estimate the occupancy in one zone. Lee et al. (2014) used a dynamic neural network model to estimate the occupancy in a single zone using CO_2 and absolute humidity measurements. Gruber et al. (2014) specifically investigated the time-delay aspect of CO_2 sensors. For a review of occupancy sensing systems and modelling approaches, the authors refer to (Yang et al., 2015).

These studies typically focus on single, small zones. Practical applications like office buildings however require the occupancy in multiple zones to be estimated. Furthermore in practical applications no specialised measurement data is available and therefore the occupancy estimation technique preferably only uses sensors that are already available. Finally, in real buildings CO_2 sensor drift may occur, causing the measurements to be biased. The measurement estimation technique should be robust against this drift.

In this paper we present a multi-zone occupancy estimation technique for office buildings equipped with Variable Air Volume (VAV) units that only uses CO_2 measurements and VAV control signals for each zone. It may be extended to other ventilation systems as long as the ventilation system may be simulated. The difference with (Ebadat et al., 2015) is that our technique does not require more advanced mathematical concepts to be implemented. It does however require a model of the building air flow network. In this work this model was developed and implemented using Modelica. The required models are presented and available open source. Occupancy estimation results are validated using measurement data for a single zone. Occupancy estimations of the 22 other zones are verified using periods of known absence like holidays.

System description

The methodology proposed in this paper is applied to measurement data from an office building in Luxembourg. In this section the relevant aspects of the building are presented.

The office building has 7000 m^2 of conditioned floor space spread over six floors. The top and bottom floors are not considered in this paper since they have their own air handling units. Ventilation to the four middle floors is provided by two air handling units (AHU) that each have a nominal volumetric flow rate of 14200 m^3/h. The supply and return volumetric flow rates of each AHU are measured. The first and second AHU respectively provide ventilation to 15 zones at the east of the building and 8 zones at the west of the building. Each zone is equipped with a supply and a return VAV such that the supply and return air mass flow rates are balanced. The supply and return VAVs are respectively of the TVZ 160 and TVA 160 series of TROX Technik. The nominal flow rate of the eastern zones is either 583 m^3/h or 1167 m^3/h, while the nominal flow rate of the western zones is 1750 m^3/h. Each VAV is configured to have a nominal flow rate of 583 m^3/h such that each zone has either one, two or three parallel VAVs.

Figure 1 illustrates that air enters the zone through multiple inlets in a suspended floor. One duct per VAV is used for air extraction. These ducts contain a

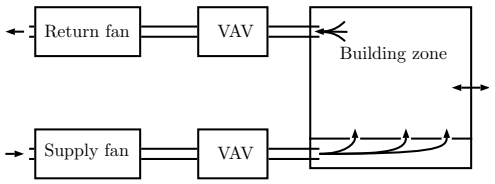

Figure 1: Schematic presentation of the building zone. Arrows indicate air flows. Air enters the zone from many small vents in the floor and leaves the zone through a few large vents at the top of each zone.

CO_2 concentration sensor, a relative humidity sensor and a temperature sensor. Windows may be opened. The building n50 value equals 0.24/h and was measured using a blower door test.

Measurement data was collected through the building management system. The measurement precisions are 1 m^3/h and 0.1 ppm. Sensor type, accuracy or calibration are unknown. Sensor measurements are stored together with a MySQL timestamp when the difference with the previous measurement value exceeds a certain threshold. In practice this means that on average one sample is stored every minute for the volumetric flow rate and for the CO_2 concentration sensors. When multiple measurements are stored within the same second, the oldest samples, i.e. with the lowest MySQL primary key values, are discarded. The resulting data is interpolated using zero-order hold based interpolation. The interpolated signal is then resampled to 2-minute averaged data by computing the average of 15 equidistant samples of the interpolated data within each 2-minute interval. The resulting data is used in the simulations, where the data is linearly interpolated.

The goal of this paper is to estimate the occupancy profiles in each of the building zones using the above information and available measurement sensors.

Methodology

In this work CO_2 sensor measurements are combined with an air flow model to estimate the occupancy in each zone using Equation (1), which requires the mass flow rate to each zone to be known. Since flow meters are typically not installed for each zone, a simulation model of the air flow network is used to compute these mass flow rates, based on the measurement data and control set points that are available. The most important component of this air flow network is the model of a VAV unit, for which a model needed to be developed and which has been published in the Modelica Annex 60 library (Wetter et al., 2015), which is further maintained as part of IBPSA project 1.

Therefore this section firstly describes the used Variable Air Volume (VAV) model and secondly the used air flow system model. Thirdly, the CO_2 sensor calibration approach is discussed. Finally, we explain how the occupancy profiles are computed.

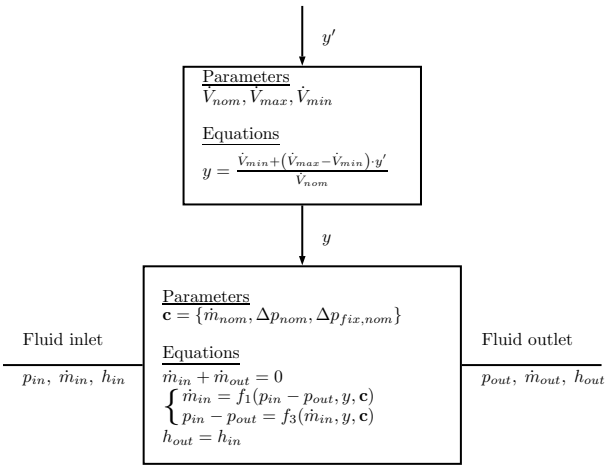

Figure 2: Schematic presentation of VAV model. The top type-specific part transforms the VAV input y' into the type-independent model input y. Important pressures p, mass flow rates $\dot{m}$, specific enthalpies h, control signals y, functions $f(\cdot)$ and equations are indicated in this scheme.

VAV model description

The considered office building uses VAV boxes to control the volumetric flow rates that enter the building zones. A Modelica model for this component has been developed. The VAV model is based on the TVA/TVZ series of TROX Technik and consists of two parts: a type-specific and a type-independent part (see Figure 2).

The first part is the type-specific model for the Trox TVA/TVZ unit. It transforms the VAV unit control input y' into the control signal y of a more generic model

$$y = \frac{\dot{V}_{min} + (\dot{V}_{max} - \dot{V}_{min}) \cdot y'}{\dot{V}_{nom}} \tag{2}$$

where $\dot{V}_{nom}$ is the nominal volumetric flow rate, which may be found in the manufacturer datasheet. $\dot{V}_{min}$ and $\dot{V}_{max}$ are respectively the lower and upper set point bounds of the volumetric flow rates. These values may be fixed on the VAV boxes using control knobs and are parameters of the model.

The second part of the VAV model is the type-independent model of a pressure independent valve. This model has been published in the Annex 60 library (Wetter et al., 2015) as the `TwoWayPressureIndependent` model, which is further maintained as part of IBPSA project 1. It has one control input y. The model consists of two main functions:

$$\dot{m} = f_1(\Delta p) \tag{3}$$

$$\Delta p = f_2(\dot{m}). \tag{4}$$

The first function is a pressure-drop equation that returns the mass flow rate $\dot{m}$ as a function of the pressure difference Δp over the VAV. Equation (4) is the inverse of Equation (3).

These equations describe two flow regimes. The first flow regime occurs when the VAV pressure difference is not high enough to reach the requested flow rate $\dot{V}_{set}$, i.e. even when the VAV damper is fully opened, the desired flow rate is not obtained. In other cases the second flow regime holds.

Functions (3) and (4) that combine these two regimes, should have specific properties. They must be unbounded such that one unique solution exists for every value of Δp or $\dot{m}$. The first derivative $\mathrm{d}\,\dot{m}/\mathrm{d}\,\Delta p$ of the function must also be continuous, since otherwise a Modelica simulation tool's Newton solver may not be able to robustly solve algebraic loops containing this function.

In the first regime, the unit is unable to supply the requested volumetric flow rate. In this case the volumetric flow rate is determined using a quadratic pressure drop equation:

$$f_3(\Delta p, k) = \dot{m} = k\sqrt{\Delta p} \tag{5}$$

$$f_4(\dot{m}, k) = \Delta p = (\dot{m}/k)^2 \tag{6}$$

where k is determined using Equation (7), with nominal mass flow rate $\dot{m}_{nom}$ and nominal pressure drop Δp_{nom} of the unit when the damper is fully opened.

$$k = \frac{\dot{m}_{nom}}{\sqrt{\Delta p_{nom}}} \tag{7}$$

$\dot{m}_{nom}$ and Δp_{nom} are parameters of the model that need to be set by the user. These values can typically be found in the datasheet of the manufacturer.

The second regime is active when $\Delta p > \Delta p_{min}$, where Δp_{min} is the minimum pressure difference required for supplying $\dot{V}_{set}$. Using (6), we find $\Delta p_{min} = (\rho \cdot \dot{V}_{set}/k)^2$. In the second regime the VAV valve restricts the flow rate by closing the damper such that $\dot{V}_{set}$ is obtained. In this region Equation (3) is equivalent to Equation (8).

$$\dot{m} = \rho \cdot \dot{V}_{set} \tag{8}$$

This equation however does not contain Δp, meaning that Δp may be undefined and therefore it is impossible to construct (4). Therefore a different approach is required, reflecting that the mass flow rate rises further when $\Delta p > \Delta p_{min}$ in the second flow regime.

A function that satisfies this requirement, that is unbounded and has a continuous first derivative is

$$\begin{aligned} \dot{m} = RS(&\Delta p - \Delta p_{min}, \\ &\dot{m}_{set} + l(\Delta p - \Delta p_{min})\dot{m}_{nom}/\Delta p_{nom}, \\ &f_3(\Delta p, k) \\ &\delta) \end{aligned} \tag{9}$$

where $\dot{m}_{set} = \rho \cdot \dot{V}_{set}$ and l is a parameter that determines the slope of $\dot{m}(\Delta p)$ in region 2. $RS(a, b, c, d)$

is a transition function that returns b for $a \geq d$, c for $a \leq -d$ and otherwise Equation (10),

$$(a/d)((a/d)^2 - 3)(c - b)/4 + (c + b)/2 \tag{10}$$

which is a transition between b and c with a continuous first derivative.
Similarly function $f_2(\cdot)$ in Equation (4) is defined using Equation (11).

$$\begin{aligned}\Delta p = RS(&\dot{m} - \dot{m}_{set},\\ &\Delta p_{min} + (\dot{m} - \dot{m}_{set})\Delta p_{nom}/\dot{m}_{nom}/l_2,\\ &f_4\dot{m}, k,\\ &\delta)\end{aligned} \tag{11}$$

Functions $f_3(\cdot)$ and $f_4(\cdot)$ represented by Equation (9) and Equation (11) are implemented in a dedicated valve model in the Annex 60 library (Wetter et al., 2015): `Annex60.Fluid.Actuators.Valves.TwoWayPressureIndependent`. This model also contains the option to model a series pressure drop component with a fixed k value k_{fixed}. Variable k is then recomputed using (12).

$$k' = \sqrt{1/(1/k_{fixed}^2 + 1/k^2)} \tag{12}$$

This option allows modelling of two pressure drop components using a single equation and therefore may result in smaller algebraic loops that may be solved more efficiently.

Air flow model description

Figure 3 illustrates the air flow network, in which mass flows from left to right. Table 1 explains the components used in Figure 3. The considered office building has 23 zones, for which air is supplied by two independent air handling units (AHU).
Each zone is modelled using two air volumes in which air is assumed to be perfectly mixed. These are illustrated for completeness, but do not affect the pressure drop in the system.
The supply and return air flow rates are controlled using two independent VAVs per zone. Any imbalance in supply and demand is compensated by drawing fresh air from the 'environment' into the bottom volume. Air flow between zones is neglected in this study because its magnitude is difficult to estimate and highly depends on whether or not windows are opened, which is an unknown function of time. Each AHU is connected to four VAVs 'valBat' that extract air from the bathrooms. They have a constant set point of 150 m^3/h each. Since no air is injected in these rooms an imbalance exists. It is assumed that this air is drawn from the environment and not from the surrounding zones.
The required duct pressure is provided by fans, but is simulated by setting an absolute pressure boundary condition using the `Boundary` models in the schematic presentation. The environment has a constant pressure of 1 atm.

Air flow model configuration

A few experiments were conducted to estimate some of the model parameters.

$\dot{V}_{max}$ and $\dot{V}_{min}$

The nominal pressure drops of 'resSup' and 'resRet' and the series pressure drop of the VAVs were calibrated using measurement data. The set points of the VAV set by the control knobs were inspected visually on a few VAVs, from which the minimum and maximum opening $\dot{V}_{min}$ and $\dot{V}_{max}$ were respectively found to be about $\sim 30\%$ and $\sim 65\%$ of $\dot{V}_{nom}$.
Further calibration of a few % was conducted using measurement data. The calibration consists of firstly deriving the values of $\dot{V}_{max}$ using an experiment where all VAVs were opened ($y' = 1$). In a second experiment all VAVs were closed ($y' = 0$), from which $\dot{V}_{min}$ could be computed. This experiment was conducted separately for both AHUs and separately for return and supply ducts.

Duct pressure drops

The pressure drop of the main ducts and the pressure drop $\Delta p_{fix,nom}$ in series with the VAVs were deduced from experiments. The series pressure drop is caused by vents, ducts, flexible ducts, bends and also a heating coil for the supply VAV. For this calibration we used 1) measurements during operation and 2) the fact that the supply pressure was set too low to reach the flow rate set point. The measured flow rate in the duct is thus lower than the sum of the requested flow rates for that duct $\sum \dot{m}_{set}$. These flow rates may be computed using the logged VAV control signals. The knowledge that the set point is not obtained means that the VAV dampers are completely opened. The pressure drop of the VAV may then be computed from Equation (6). The model was fit using trial and error to attribute the remaining pressure drop to the main duct and the series pressure drop of the VAVs.

Similar pressure drops for the return ducts needed to be deduced. The return ducts contain no heating coil, due to which their pressure drop is lower. Therefore the return duct pressure difference was high enough and the trick of the supply ducts could not be used to deduce the pressure drop of the series components. However, on some occasions the nominal mass flow rate of one of the two return fans was reached. To protect the filters, the fan controller then lowers the duct pressure to avoid exceeding the nominal mass flow rate. Due to this effect the first operating region of the VAVs is again reached, meaning that the pres-

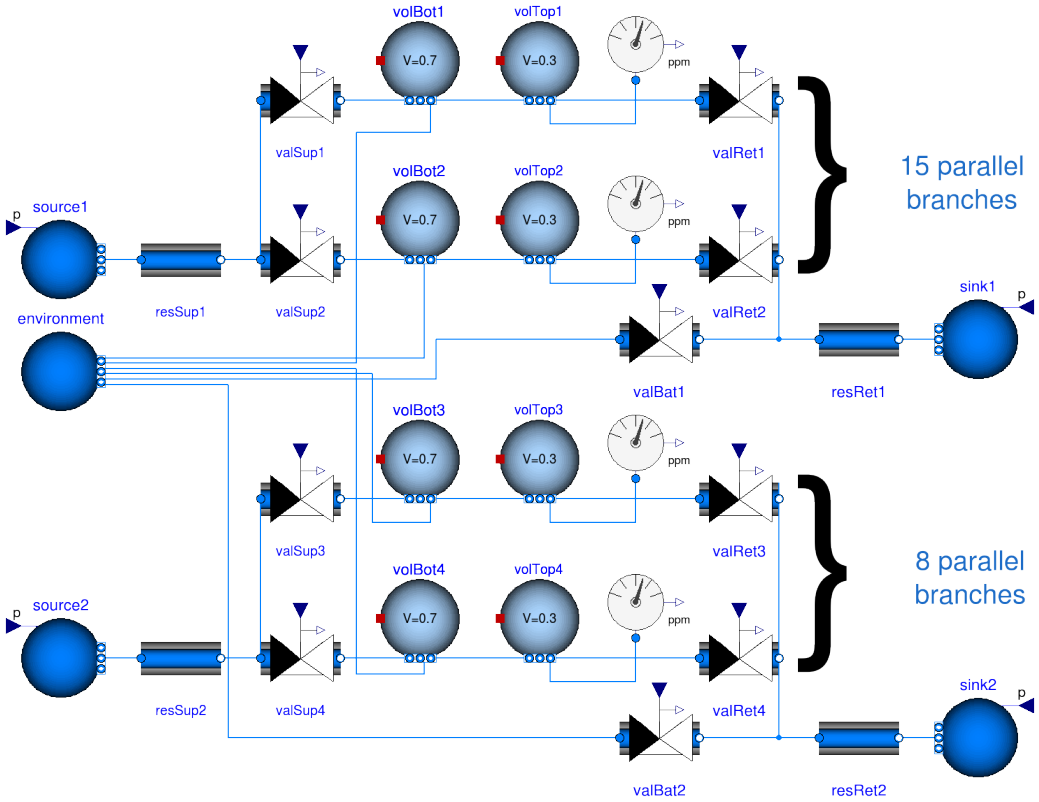

Figure 3: Illustration of the air flow network containing two independent duct systems that supply air to respectively 15 and 8 zones from which 2 are shown. Each zone contains two air volumes, one supply and one return VAV 'valSup' and 'valRet'. The ducts are represented using pressure drop components resSup and resRet. Boundary 'environment' sets the absolute pressure in the zones to 1 atm. Any mass flow rate imbalance in the supply and return VAVs is compensated by a mass flow rate to or from the environment. The bathrooms contain only VAVs for extracting air. It is assumed that this air is drawn from the environment. Table 1 explains the used symbols.

Table 1: Table explaining the components used in Figure 3 and their sources.

Icon	Description	Source
	`VAV model`: The VAV model outlined in this paper.	Custom
	`FixedResistanceDpM`: Pressure drop element that sets $\Delta p = \left(\frac{\dot{m}}{k}\right)^2$ or $\dot{m} = k \cdot \sqrt{\Delta p}$ with k defined using Equation (7).	Annex 60 (Wetter et al., 2015)
	`Boundary`: Serves as a mass source or sink by setting a pressure boundary condition to the connected model.	Annex 60 (Wetter et al., 2015)
	`CO2 sensor`: Measures the CO_2 concentration in the connected component.	Annex 60 (Wetter et al., 2015)
	`MixingVolume`: This component perfectly mixes all entering mass streams but causes no pressure drop.	Annex 60 (Wetter et al., 2015)

sure drops could again be deduced from the measured return duct pressure.
The pressure drops for the *other* return duct system were chosen equal to the values of the return duct system where the above described automatic pressure reduction occurred because no better estimate could be deduced.

The supply and return series pressure drops for the VAV maximum flow rate of 591 m^3/h were found to be respectively 215 Pa and 43 Pa for the AHU with 8 VAVs and 258 Pa and 43 Pa for the AHU with 15 VAVs. The supply and return main duct pressure drops for the (different) duct nominal flow rate of 14200 m^3/h were found to be respectively 86 Pa and 30 Pa for the AHU with 8 VAVs and 108 Pa and 30 Pa for the AHU with 15 VAVs. The higher main supply duct pressure drop compared to the main return duct pressure drop may be explained by the presence of a humidifier in the main supply ducts.

Occupancy estimation methodology

To compute the zone occupancy, Equation (1) is used, which may be reformulated into Equation (13)

$$\frac{\mathrm{d}\, c(t)}{\mathrm{d}\, t} = \frac{(c_{ext} - c(t))\frac{\dot{m}}{\rho_{air}} + n(t) \cdot G \cdot 10^6}{V} \tag{13}$$

where n is the number of occupants and G is the CO_2 generation rate per person. In literature often a CO_2 generation rate of 0.3 l/min or 0.31 l/min per person is used (Mumma, 2004; Wang et al., 1999; Dougan and Damiano, 2004; Lu et al., 2010). This generation rate however led to an overestimation of the occupancy. The generation rate was therefore computed assuming an average heat production of $\sim$ 21 J (5 kcal) per liter of O_2 that is consumed (Hills et al., 2014). Assuming a respiratory quotient of 1 and a heat production rate of 131 W, which corresponds to 'Moderately active office work' (American Society of Heating and Engineers, 2009), we find a generation rate of 0.38 l/min. Ebadat et al. (2015) use a generation rate of 0.48 l/min.

To compute the occupancy profile for each VAV, equation (13) was solved towards $n(t)$.

$$n(t) = \frac{V\frac{\mathrm{d}\, c(t)}{\mathrm{d}\, t} + (c(t) - c_{ext})\frac{\dot{m}}{\rho_{air}}}{G \cdot 10^6} \tag{14}$$

This results into Equation (14) where $\dot{m}$ is computed using the described air flow model, $c(t)$ is the calibrated value of the two-minute time-averaged measured indoor CO_2 concentration $c'(t)$ and $\frac{\mathrm{d}\, c(t)}{\mathrm{d}\, t}$ is computed approximately using the Modelica model `Modelica.Blocks.Continuous.Derivative` with parameter value T = 600 s.
The exterior CO_2 concentration $C_{ext}$is not measured on site. Therefore measurements from 8 often unoccupied meeting rooms and offices were combined to serve as the outdoor CO_2 concentration. The zone volume V was computed from the zone geometry. The air density ρ_{air} is assumed to be constant and equal to 1.204 kg/m^3. G is taken as 0.38 l/min as computed above.

CO_2 sensor calibration

The used CO_2 sensors experience a drift on the measured concentration, which needs to be removed. Automatic Baseline Calibration (ABC) is often used for removing this measurement error by adding a fixed offset to the measured value. ABC stores the lowest CO_2 concentration c_{min} that is measured during a certain period. The method assumes that c_{min} is equal to the constant outdoor CO_2 concentration c_{out} = 400 ppm. The measured CO_2 concentration $c'(t)$ is then calibrated in the next period by computing the calibrated value $c(t)$ using Equation (15).

$$c(t) = c'(t) + c_{out} - c_{min} \tag{15}$$

For our case ABC is however unsuited since large outdoor CO_2 concentration swings are observed so assuming a constant value would be inappropriate. Figure 4a illustrates these swings using four CO_2 measurements and the outdoor wind speed during seven days starting on Thursday. Some of the meeting rooms were occupied on Friday noon and Monday noon. Outside of these periods we assume that the measured CO_2 concentrations may be used as an indicator for the outdoor CO_2 concentration, for which no sensor is available. Figure 4a shows that the outdoor CO_2 concentration experiences fluctuations of up to 100 ppm, especially during periods of low wind speeds.
Furthermore Figure 4b shows that on some occasions the indoor CO_2 concentration drops below the outdoor CO_2 concentration, since the CO_2 concentration rises when the AHU is activated. This suggests that something in the room absorbs CO_2, for which no conclusive cause could be identified. Using ABC in this situation would lead to a large underestimation of the outdoor CO_2 concentration.
From these observations we conclude that ABC calibration would not be reliable in this study. Therefore Equation (16) is used to correct for the drift on the CO_2 sensors where $c'(t_0)$ is the CO_2 concentration that is measured at time t_0, which is the last date when there was a national holiday. During these periods the building is assumed to be unoccupied, while the ventilation is still running. Therefore all CO_2 sensors may be calibrated to the same CO_2 concentration.

$$c(t) = c'(t) + c_{out} - c'(t_0) \tag{16}$$

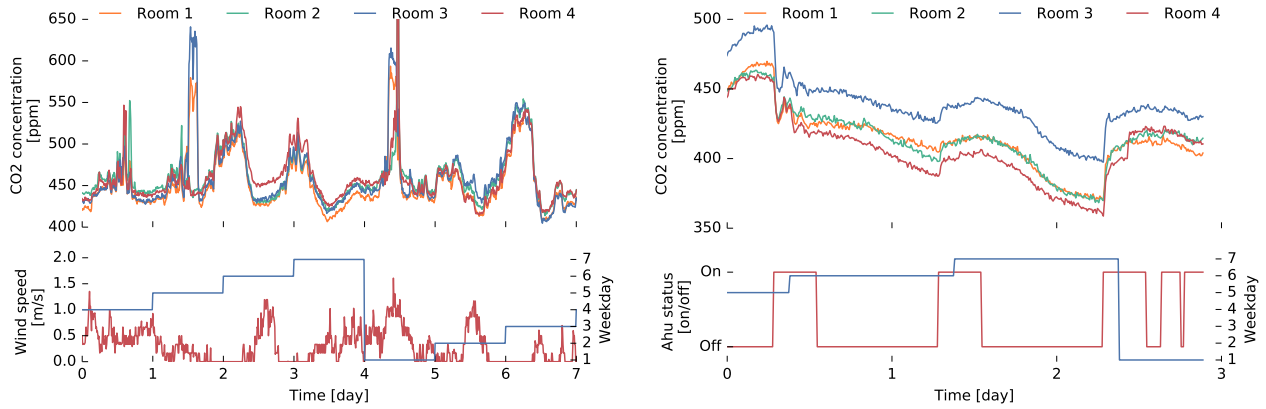

(a) The ventilation unit was activated throughout the illustrated week. Therefore each measurement is indicative of the outdoor CO_2 concentration.

(b) Measurement results during a weekend where the air handling unit (AHU) is only activated at night.

Figure 4: Calibrated CO_2 measurements of four meeting rooms that are usually unoccupied.

Validation results

Air flow model validation

The air flow model was validated using volumetric flow rate measurements from the building and using the control signals of the VAVs. The validation results are shown in Figure 5, which shows the measured and simulated return and supply mass flow rates of the two AHUs and the measured boundary conditions for the duct pressures that were used. The end of the graph shows an experiment where groups of VAVs were opened sequentially by changing $y' = 0$ to $y' = 1$. The maximum steady state error is in the order of 5%.

Note that the supply air flow rate is significantly lower than the return mass flow rate because the duct pressure set point is too low. This is correctly simulated.

Occupancy estimation validation

Using the validated air flow model, the zone mass flow rates were computed and Equation (14) was used to compute the number of occupants in all zones. One of the zones was validated using measurements. To this end a bi-directional people counter was installed at the entrance of the zone as illustrated in Figure 6. The counter comprises two parts. The first part contains a led and the second contains two light sensors. When a person blocks the light coming from the LED, a log entry is made that contains a time stamp and which of the two sensors' view was blocked first. Based on these logs the occupancy was computed. Occasionally measurement errors occurred such that the measured number of occupants at the end of the day is not zero. Therefore the counter is reset to zero each night. The zone consists of two smaller zones with 1 and 2 VAVs such that the zone has three VAVs in total.

Figure 7 shows the validation results. The top graph depicts the measured and estimated occupancy profiles. The middle graph shows the measured control signals y' for each of the three VAVs. Note that $y' = 0$ corresponds to a valve opening of $y \approx 0.5$. The AHUs are disabled at night when $y' = 0$ such that the mass flow rate then equals zero. The bottom graph shows the measured zone CO_2 concentration and the exterior CO_2 concentration.

Discussion

Qualitatively the occupancy estimation agrees well with the measured values. Figure 8 shows results of a single week that allows for a more detailed discussion. Figure 8 shows that at the end of each day the total number of people entering and leaving the zone does not add up to zero. Although the differences are typically $\pm$ 1 person, this indicates that some measurement errors exist that should be taken into account when interpreting the results.

The measurements indicate that many people leave the office at noon. This is also detected by the occupancy estimator but the occupancy minimum is typically underestimated and delayed by about an hour by the inertia of the room air.

It often happens that the ventilation unit is disabled in the evening before all CO_2 has been evacuated. The remaining CO_2 concentration then drops throughout the night but in the morning the remaining CO_2 concentration is higher than the exterior CO_2 concentration, causing the algorithm to erroneously detect occupancy as soon as the ventilation unit is enabled. This may of course be avoided by running the AHU longer or until the CO_2 concentration drops below a certain value.

Around noon of day 5 the ventilation unit was disabled for about one hour, causing the CO_2 concentration in the building to rise. Although this effect was taken into account when computing the VAV mass flow rate, this still leads to a peak occupancy prediction for a short period when the AHU was re-enabled.

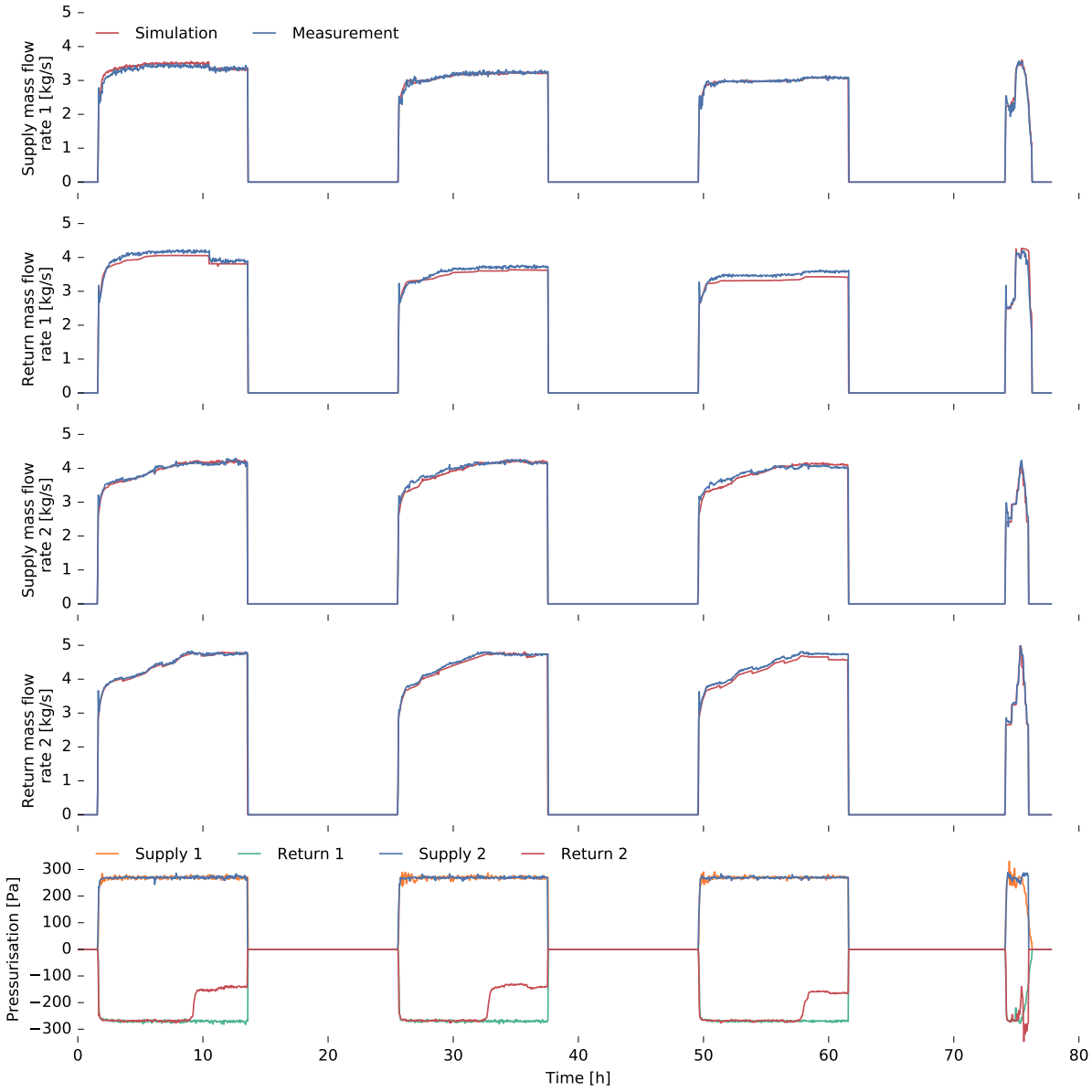

Figure 5: Validation of air flow network. The four top sub-graphs compare the simulated mass flow rates with the measured mass flow rates for the pressure differences indicated in the bottom sub-graph.

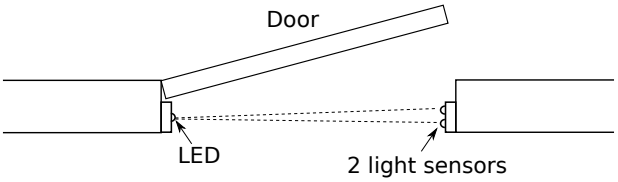

Figure 6: Illustration of people counter comprising a part that contains a LED and a part that contains two light sensors.

The order of magnitude of the occupancy is well predicted. This indicates that G = 0.38 l/min is an appropriate average CO_2 generation rate for this study. Figure 7 shows that the measured zone CO_2 concentration decays towards the outdoor CO_2 concentration during weekends, indicating that the calibration method works as intended.

The main steps forward in this research in relation to existing literature are the use of 1) a long validation period, 2) only pre-existing sensors, 3) a large number of occupants, 4) a real office environment. Our approach can estimate the occupancy of each zone for which a return CO_2 concentration sensor is installed and for which the ventilation mass flow rate is measured or may be computed using a model. The CO_2

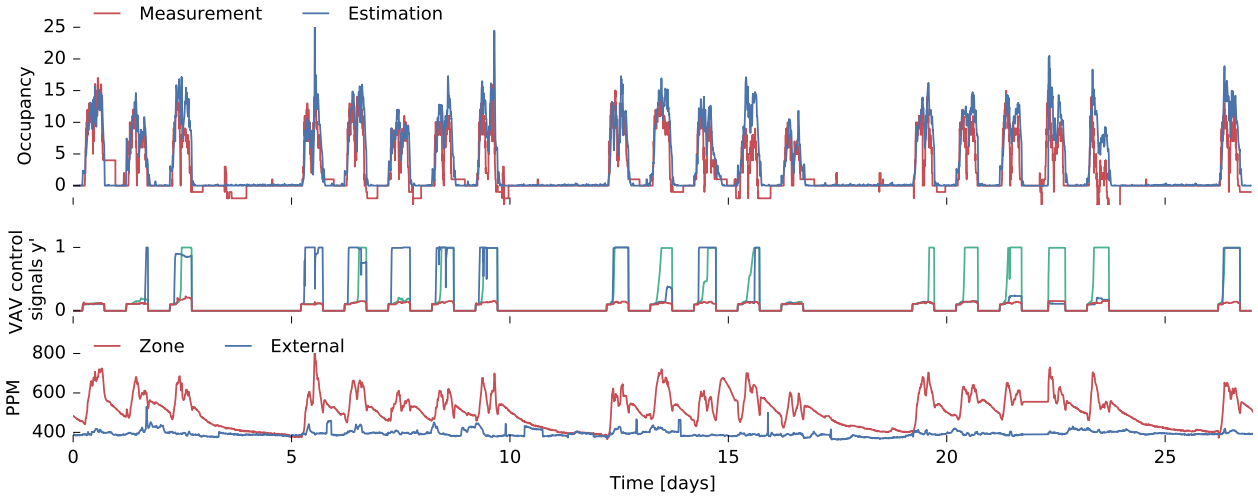

Figure 7: Validation of occupancy estimation approach for one zone with three supply VAVs. The measured and estimated occupancy are on the top graph. The middle graph shows the VAV control signals y'. The bottom graph shows the measured zone CO_2 concentration and the computed outdoor CO_2 concentration.

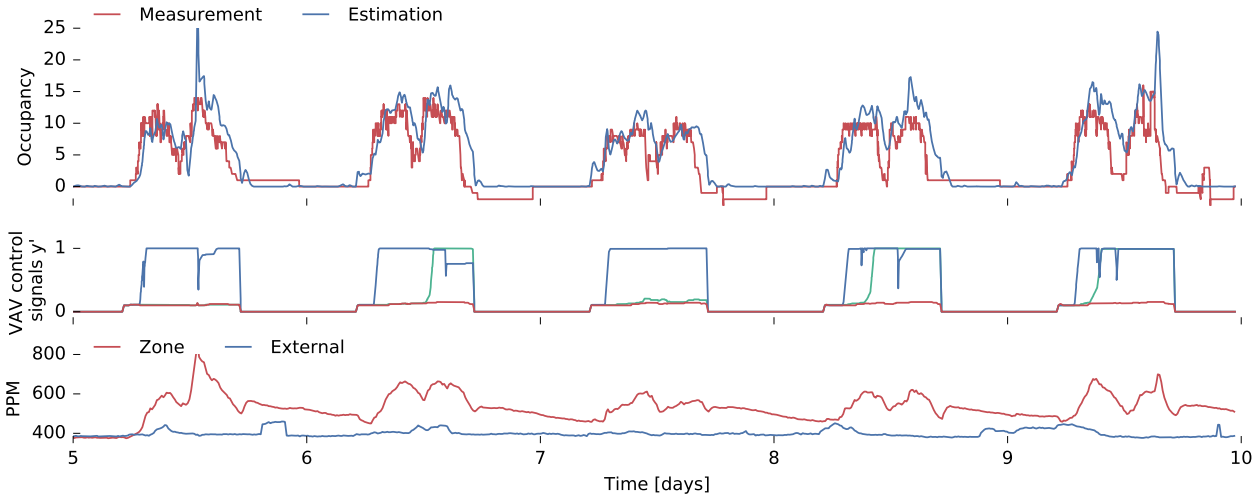

Figure 8: More detailed illustration of the validation in Figure 7 for a single week (Monday - Friday).

sensor calibration approach compensates for sensor drift and makes the approach robust against fluctuations of the outdoor CO_2 concentration.

Conclusion

A direct approach for estimating occupancy profiles in buildings by using readily available sensors has been implemented and validated using measurement data from a real office building during operation. Due to the limited number of available measurements the outdoor CO_2 concentration needed to be estimated and a validated air flow model was used to compute the zone air flow rates. To this end a new VAV model has been developed, which is published in the Annex 60 library (Wetter et al., 2015). The limitations of Automatic Baseline Calibration for this study were shown and an alternative calibration method has been used.

Validation results show that the Modelica model is able to accurately compute the total mass flow rates in the air flow system, proving the validity of the model and demonstrating the use of Modelica to perform detailed building air flow calculations. The occupancy predictions agree well with the measured occupancy profile of a single zone and can be used to estimate the internal gains of the building during building performance simulations or advanced controller assessments. A CO_2 generation rate of 0.38 l/min per person was computed and yields better results compared to the typically used value of 0.3 l/min.

Acknowledgement

The authors wish to thank Michael Wetter for his feedback on the VAV model and for his development of the Buildings and Annex 60 libraries, which greatly facilitated the development of the presented model.

We thank Sensor Development International B.V. for providing the people counter and Schuler immo, DRC Technology and Boydens Engineering for providing the measurement data that was used in this work. This research was supported by the Agency for Innovation by Science and Technology in Flanders (IWT) under Grant 131012. This research emerged from collaborations within the Annex 60 project, an international project conducted under the umbrella of the International Energy Agency (IEA) within the Energy in Buildings and Communities (EBC) Programme. Annex 60 develops and demonstrates new generation computational tools for building and community energy systems based on Modelica, Functional Mockup Interface and BIM standards.

References

American Society of Heating, R. and A.-C. Engineers (2009). *2009 ASHRAE Handbook: Fundamentals*. 2009 Ashrae Handbook - Fundamentals. American Society of Heating, Refrigeration and Air-Conditioning Engineers.

Ansanay-Alex, G. (2013). Estimating Occupancy Using Indoor Carbon Dioxide Concentrations Only in an Office Building: a Method and Qualitative Assessment. In *REHVA World Congress on Energy efficient, smart and healthy buildings (CLIMA)*, Prague.

Calì, D., P. Matthes, K. Huchtemann, R. Streblow, and D. Müller (2015). CO_2 based occupancy detection algorithm: Experimental analysis and validation for office and residential buildings. *Building and Environment 86*, 39–49.

Dougan, D. S. and L. Damiano (2004). CO 2 -Based Demand Control Ventilation: Do Risks Outweigh Potential Rewards? *ASHRAE Journal 46*(10), 47–53.

Ebadat, A., G. Bottegal, M. Molinari, D. Varagnolo, B. Wahlberg, H. Hjalmarsson, and K. H. Johansson (2015). Multi-room occupancy estimation through adaptive gray-box models. In *IEEE Conference on Decision and Control*, Osaka.

Gruber, M., A. Trüschel, and J.-O. Dalenbäck (2014). CO_2 sensors for occupancy estimations: Potential in building automation applications. *Energy and Buildings 84*, 548–556.

Han, Z., R. X. Gao, and Z. Fan (2012). Occupancy and indoor environment quality sensing for smart buildings. In *2012 IEEE International Instrumentation and Measurement Technology Conference Proceedings*, Graz, pp. 882–887.

Hills, A. P., N. Mokhtar, and N. M. Byrne (2014). Assessment of physical activity and energy expenditure: an overview of objective measures. *Frontiers in Nutrition 1*(5), 1–16.

Lee, J.-y., H. Han, K.-j. Jang, J.-d. Chung, and H. Hong (2014). Carbon dioxide and humidity data in estimating occupancy using dynamic neural network model. In *Roomvent 2014*, Sao Paulo.

Lu, T., A. Knuutila, M. Viljanen, and X. Lu (2010). A novel methodology for estimating space air change rates and occupant CO_2 generation rates from measurements in mechanically-ventilated buildings. *Building and Environment 45*(5), 1161–1172.

Mumma, S. A. (2004). Transient Occupancy Ventilation By Monitoring CO_2. *IAQ Applications 5*(1), 21–23.

Pérez-Lombard, L., J. Ortiz, and C. Pout (2008, jan). A review on buildings energy consumption information. *Energy and Buildings 40*(3), 394–398.

Wang, S., J. Burnett, and H. Chong (1999). Experimental Validation of CO_2-Based Occupancy Detection for Demand-Controlled Ventilation. *Indoor and Built Environment 8*(6), 377–391.

Wetter, M., M. Fuchs, P. Grozman, L. Helsen, F. Jorissen, M. Lauster, M. Dirk, C. Nytsch-geusen, D. Picard, P. Sahlin, and M. Thorade (2015). IEA EBC Annex 60 Modelica Library - An International Collaboration to Develop a Free Open-Source Model Library for Buildings and Community Energy Systems. In J. Mathur and V. Garg (Eds.), *Building Simulation 2015*, Hyderabad, India.

Yang, J., M. Santamouris, and S. E. Lee (2015). Review of occupancy sensing systems and occupancy modelling methodologies for the application in institutional buildings. *Energy and Buildings 121*, 344–349.